THE JOURNAL OF BIOLOGICAL CHEMISTRY
Vol. 279, No. 13, Issue of March 26, pp. 12051–12059, 2004

Printed in U.S.A.

p38^{MAPK} Acts in the BMP7-dependent Stimulatory Pathway during Epithelial Cell Morphogenesis and Is Regulated by Smad1*

Received for publication, September 23, 2003, and in revised form, January 8, 2004
Published, JBC Papers in Press, January 12, 2004, DOI 10.1074/jbc.M310526200

Ming Chang Hu, David Wasserman, Sunny Hartwig, and Norman D. Rosenblum‡

From the Division of Nephrology, Program in Developmental Biology, The Hospital for Sick Children, University of Toronto, Toronto, Ontario M5G 1X8, Canada

Bone morphogenetic protein (BMP)-7 exerts dose-dependent stimulatory and inhibitory effects during renal branching morphogenesis. Previously, we identified an inhibitory role for activin-like kinase receptors and Smad1 in BMP-dependent inhibition (Piscione, T. D., Phan, T., and Rosenblum, N. D. (2001) *Am. J. Physiol.* 280, F19–F33). Here we demonstrate a novel role for p38 mitogen-activated kinase (p38^{MAPK}) in BMP7-dependent stimulatory signaling. Stimulatory doses (0.25 nM) of BMP7 increased p38^{MAPK} activity and stimulated phosphorylation of endogenous activating transcription factor 2 (ATF2) in a p38^{MAPK}-dependent manner in murine inner medullary collecting duct (mIMCD-3) cells. In contrast, high doses (10 nM) of BMP7 inhibited p38^{MAPK} activity and phosphorylation of endogenous ATF2. Treatment with BMP7 exerted no significant effect on the levels of the phosphorylated forms of endogenous SAPK/JNK or p44 and p42 (ERK1 and ERK2) protein kinases. To investigate the functional importance of p38^{MAPK} signaling, we showed that SB203580, a p38^{MAPK} inhibitor, blocked the stimulatory effect of BMP7 on mIMCD-3 cell morphogenesis but had no effect on BMP7-dependent inhibition in a three-dimensional culture model. To identify mechanisms by which BMP7-dependent inhibitory signaling suppresses p38^{MAPK} activity, we measured p38^{MAPK} activity in ligand independent mIMCD-3 models of enhanced and suppressed Smad signaling. Basal activity of p38^{MAPK} was decreased in mIMCD-3 cells and in embryonic kidney tissue expressing a constitutively active activin-like kinase receptor, but was increased in mIMCD-3 cells stably expressing a dominant negative form of Smad1. We conclude that BMP7 stimulates renal epithelial cell morphogenesis via p38^{MAPK} and that p38^{MAPK} activity is negatively regulated by Smad1.

Renal branching morphogenesis, defined as growth and branching of epithelial tubules during embryogenesis, is dependent on reciprocal inductive tissue interactions between the mesenchymal metanephric blastema and the epithelial ureteric bud and its daughter collecting ducts. These interactions are mediated, in part, by secreted growth factors and their cognate signaling effectors. Bone morphogenetic protein (BMP)[1]-7, a member of the transforming growth factor (TGF)-β superfamily, modulates renal branching morphogenesis, consistent with its spatial expression pattern during branching morphogenesis (1) and the arrested branching phenotype observed in *Bmp7* null mice (2, 3). The response of ureteric bud and collecting duct cells to BMP7 is complex and distinct from that of other members of the TGF-β superfamily. BMP7 exerts dose-dependent and opposite effects on ureteric bud morphogenesis in embryonic kidney explants treated with BMP7-agarose beads and in the murine inner medullary collecting duct (mIMCD-3) cell culture model (4, 5). In contrast, BMP2, a related TGF-β superfamily member expressed during renal embryogenesis, only inhibits ureteric bud and collecting duct morphogenesis in a monophasic dose-dependent manner (4). These findings suggest that BMP7 acts via distinct intracellular signaling pathways to exert stimulatory and inhibitory effects.

BMPs initiate intracellular signaling after binding to cell surface type I (activin-like kinase (ALK)) and type II serine/threonine kinases. Upon ligand binding, the type II receptor, BMPRII, transphosphorylates and activates the ALK receptor. ALK receptors signal via Smad proteins and mitogen-activated protein kinases (MAPK). Activation of the ALK receptor leads to association and phosphorylation of a receptor-activated Smad protein. Phosphorylation induces the receptor-activated Smad to dissociate from the receptor, stimulates the assembly of a heteromeric complex between the phosphorylated receptor-activated Smad and the co-Smad, Smad 4, and induces nuclear accumulation of this complex (6). We have demonstrated that BMPs inhibit renal epithelial cell morphogenesis after binding ALK receptors and activating receptor-dependent Smads (7, 8). In the case of BMP7, high doses activate Smad1 and induce formation of Smad1-Smad4 molecular complexes. Suppression of Smad1 signaling by overexpression of a dominant negative form of Smad1 (Smad1$^{\Delta 458}$) abrogates the inhibitory actions of BMP7 on mIMCD-3 cell morphogenesis (5). In contrast, low doses of BMP7 fail to activate Smad1 and stimulate collecting duct morphogenesis in a manner independent of Smad1 activity (5), suggesting that BMP7-dependent stimulatory signaling occurs via a Smad1-independent pathway.

BMPs have also been shown to signal via the p38 class of MAPK in nonrenal cells (9, 10). In addition, p38^{MAPK} activity can be regulated by BMP signaling, providing a feedback mechanism to regulate the cellular response to BMPs. For example,

* This work was supported by an operating grant award by the Canadian Institutes of Health Research (to N. D. R.) and by a graduate studentship award from the Research Training Centre of The Hospital for Sick Children (to S. H.). The costs of publication of this article were defrayed in part by the payment of page charges. This article must therefore be hereby marked "*advertisement*" in accordance with 18 U.S.C. Section 1734 solely to indicate this fact.

‡ To whom correspondence should be addressed: Division of Nephrology, The Hospital for Sick Children, 555 University Ave., Toronto, Ontario M5G 1X8, Canada. Tel.: 416-813-5667; Fax: 416-813-6271; E-mail: norman.rosenblum@sickkids.ca.

[1] The abbreviations used are: BMP, bone morphogenetic protein; ALK, activin-like kinase; SAPK, stress-activated protein kinase; JNK, c-Jun NH_2-terminal kinase; MAPK, mitogen-activated protein kinase; WT, wild type; HA, hemagglutinin; EGF, epidermal growth factor; TGF-β, transforming growth factor-β; DIC, differential interference contrast; ATF2, activating transcription factor 2.

in MH60 cells, the ALK receptor inhibitor, Smad6, blocks BMP2-induced activation of p38^{MAPK} (11). Because Smad6 functions by inhibiting activation of receptor-activated Smads by ALK receptors, this observation suggests that ALK receptors can activate p38^{MAPK}. The spatial expression of p38^{MAPK} in both the ureteric bud and metanephric blastema (12) suggests a functional role for this MAPK during kidney development. This is supported by the observation that pharmacologic inhibition of p38^{MAPK} in embryonic explants inhibits kidney growth and induces marked mesenchymal cell apoptosis (13). Although the effects of BMPs on p38^{MAPK} in the embryonic kidney are undefined, the presence of massive mesenchymal cell apoptosis in the *Bmp7* null mouse (2) suggests the possibility that loss of BMP7-dependent regulation of p38^{MAPK} could contribute to this phenotype.

In this paper, we investigated molecular mechanisms that control BMP7-dependent stimulation of collecting duct cell morphogenesis. We demonstrate that BMP7 regulates p38^{MAPK} activity in a dose-dependent manner, stimulating at high doses and inhibiting at high doses. In the mIMCD-3 cell culture model, we show that BMP7-dependent stimulation of epithelial cell morphogenesis is abrogated by pharmacologic inhibition of p38^{MAPK}. By using a ligand-independent model of BMP7 signaling in which a constitutive active form of ALK2 is stably expressed in mIMCD-3 cells, we demonstrate that ALK/Smad1 signaling negatively regulates p38^{MAPK} activity. Our observation that phosphorylation of activating transcription factor (ATF)-2, a p38^{MAPK} target, is decreased in embryonic kidneys expressing a constitutive active ALK receptor suggests that p38^{MAPK}-Smad interactions occur *in vivo*. Our results provide a molecular explanation for BMP7 dose-dependent signaling in epithelial cells. In addition, our findings suggest a mechanism controlling the biological response to increasing doses of BMP7 during renal branching morphogenesis.

EXPERIMENTAL PROCEDURES

Immunoblot and Immunoprecipitation Assays—Proteins in cell lysates were separated by SDS-PAGE, and immunoblotted. p38^{MAPK}, ATF2, SAPK/JNK, and ERK1/2 were identified with specific antibodies directed against phosphorylated or total (phosphorylated and unphosphorylated) forms (p38^{MAPK}, 1:250 dilution, Upstate Biotechnology, Inc.; ATF2, 1:500 dilution, SAPK/JNK and ERK1/2, 1:250 dilution, Cell Signaling). For assays of p38^{MAPK} activity, cell lysates were incubated with protein G-agarose (Amersham Biosciences) and anti-p38^{MAPK} antibody (Upstate Biotechnology, Inc.). After washing the immunocomplex sequentially in lysate buffer and kinase buffer (25 mM Tris-HCl, pH 7.5; 5 mM β-glycerol phosphate; 1 mM Na_3VO_4; 10 mM okadaic acid; 2 mM dithiothreitol; 10 mM $MgCl_2$), beads were incubated with kinase buffer, ATF2 protein (Cell Signaling), and [γ-^{32}P]ATP and incubated at 30 °C for 30 min. Proteins were then separated by SDS-PAGE, transferred to polyvinylidene difluoride membrane, and immunoblotted with anti-phospho-ATF2 antibody followed by anti-rabbit horseradish peroxidase (1:10,000) and chemiluminescence. For Smad1-Smad4 complex assays, cell lysates were subjected to immunoprecipitation with anti-Smad1 antibody (Upstate Biotechnology, Inc.) followed by absorption to protein A-Sepharose (Amersham Biosciences). Immunoprecipitated proteins were washed, separated by SDS-PAGE, and immunoblotted using a rabbit anti-Smad4 antibody (Upstate Biotechnology, Inc.) (1:1000 dilution) followed by anti-rabbit horseradish peroxidase (1:10,000) and chemiluminescence (7).

mIMCD-3 Culture Model of Epithelial Cell Morphogenesis—We have characterized previously the mIMCD-3 cell model of epithelial cell morphogenesis (8). Assays for formation of tubule progenitors were performed in type I collagen in 96-well culture plates as described (4). Cell culture medium was supplemented with BMP7 (provided via a material transfer agreement with Creative Biomolecules) or EGF (Roche Applied Science) in the presence or absence of SB203580 (Calbiochem). After 48 h, gels were fixed in 4% formaldehyde, washed in phosphate-buffered saline, and them imaged by differential interference contrast (DIC) microscopy. The number of linear structures in an area of standard dimensions was determined in four randomly selected positions of the gel for each treatment condition by an observer blinded to the treatment condition. Data were analyzed using the Statview statistical analysis program (version 4.01; Abacus Concepts, Berkeley, CA). The mean difference between treatment groups and control was analyzed by Student's *t* test (two-tailed).

Generation of Alk2 DNA Constructs—Plasmids (pCMV5) encoding human hemagglutinin (HA)-tagged wild-type (WT) and constitutive active (Q207D) *Alk2* receptors were kindly provided by Dr. L. Attisano (14). The HA tag region encodes a unique NheI restriction site. A double-stranded DNA linker encoding a FLAG tag flanked by 5′ NheI and 3′ BamHI restriction sites was synthesized: 5′-CGGTCTAGCTAGCGATTACAAGGACGACGATGACAAGTAAGGATCCGCGG-3′. The NheI/BamHI-digested linker was ligated to NheI/BamHI-digested *pCMV5-Alk2^{WT}-HA* or *pCMV5-Alk2^{Q207D}-HA* generating a carboxyl-terminal FLAG tag. Each insert was then excised from the pCMV vector with KpnI and SmaI and ligated to KpnI/EcoRV-digested pTRACER-SV40. Sequences of *pTRACER-SV40-Alk2^{WT}-HA-FLAG* and *pTRACER-SV40-A Alk2^{Q207D}-HA-FLAG* were confirmed by DNA sequencing.

Cell Lines and Transfection—mIMCD-3 cells were transfected with *pTRACER-SV40-Alk2^{WT}-HA-FLAG* or *pTRACER-SV40-Alk2^{Q207D}-HA-FLAG* using a calcium phosphate transfection method. Zeocin (500 μg/ml)-resistant clones that stably expressed wild-type or mutant forms of ALK2 were identified by screening protein lysates by immunoblotting. Tagged ALK2 was detected in immunoblots using a mouse monoclonal antibody to FLAG (Sigma, 1:2000 dilution) and chemiluminescence as recommended by the manufacturer (ECL kit; Amersham Biosciences). The spatial expression of tagged ALK2 was determined in cultured mIMCD-3 clones using an anti-HA monoclonal antibody (1:100 dilution) and confocal imaging as described previously (8).

Analysis of Ureteric Bud Branching in Embryonic Kidneys—Kidneys were surgically dissected from embryonic (E) day 13.5 pregnant mice and cultured as described (4). Ureteric bud-derived structures were identified in whole mount kidney specimens with fluorescein isothiocyanate-conjugated *Dolichos biflorus* agglutinin (20 μg/ml) (Vector Laboratories, Burlington, Ontario, Canada) as described. Ureteric bud branch points were defined as the intersection between two connected branches (15).

RESULTS

BMP7 Activates p38^{MAPK} in a Dose-dependent Manner—We investigated the role of p38^{MAPK} and its downstream target, ATF2, during BMP7 signaling in collecting duct cells. Like BMP7, p38^{MAPK} stimulates cell survival and proliferation in the embryonic kidney (12). The observation that p38^{MAPK} is activated by BMPs in nonrenal cells (11) suggested that p38^{MAPK} may be an effector in the BMP7 stimulatory pathway during renal branching morphogenesis. Previous findings that ATF2 is activated via phosphorylation by p38^{MAPK} during the response to altered pH in the mature kidney (16) and during signaling by ALK receptors (17) suggested ATF2 as a candidate transcriptional target of p38^{MAPK}-dependent BMP7 signaling. We measured p38^{MAPK} activity and the levels of endogenous ATF2 in collecting duct (mIMCD-3) cells treated for 1 h with low (stimulatory) or high (inhibitory) doses of BMP7 (Fig. 1). p38^{MAPK} was immunoprecipitated from the protein lysates of BMP7-treated cells and then used in an assay of ATF2 phosphorylation using exogenous ATF2 substrate. Compared with untreated cells, a stimulatory dose of BMP7 increased p38^{MAPK}-dependent phosphorylation of ATF2 1.5-fold (Fig. 1, *A* and *B*). In contrast, an inhibitory dose of BMP7 exerted no such effect. In fact, 10 nM BMP7 inhibited p38^{MAPK}-dependent phosphorylation of ATF2 1.6-fold compared with control and 2.4-fold compared with 0.25 nM BMP7 (p38^{MAPK} activity (densitometric units), control *versus* 0.25 nM BMP7, 52 ± 20 *versus* 80 ± 16, $p = 0.008$; control *versus* 10 nM BMP7, 52 ± 20 *versus* 33 ± 12, $p = 0.048$). Analysis of the total quantity of immunoprecipitated p38^{MAPK} and ATF2 added to each assay demonstrated that changes in phospho-ATF2 were not attributable to variation in the quantity of these proteins. Consistent with the dose-dependent stimulatory and inhibitory effects of BMP7 on p38^{MAPK} activity, a stimulatory dose of BMP7 increased phosphorylation of p38^{MAPK} 1.6-fold (Fig. 1, *A* and *B*). In contrast,

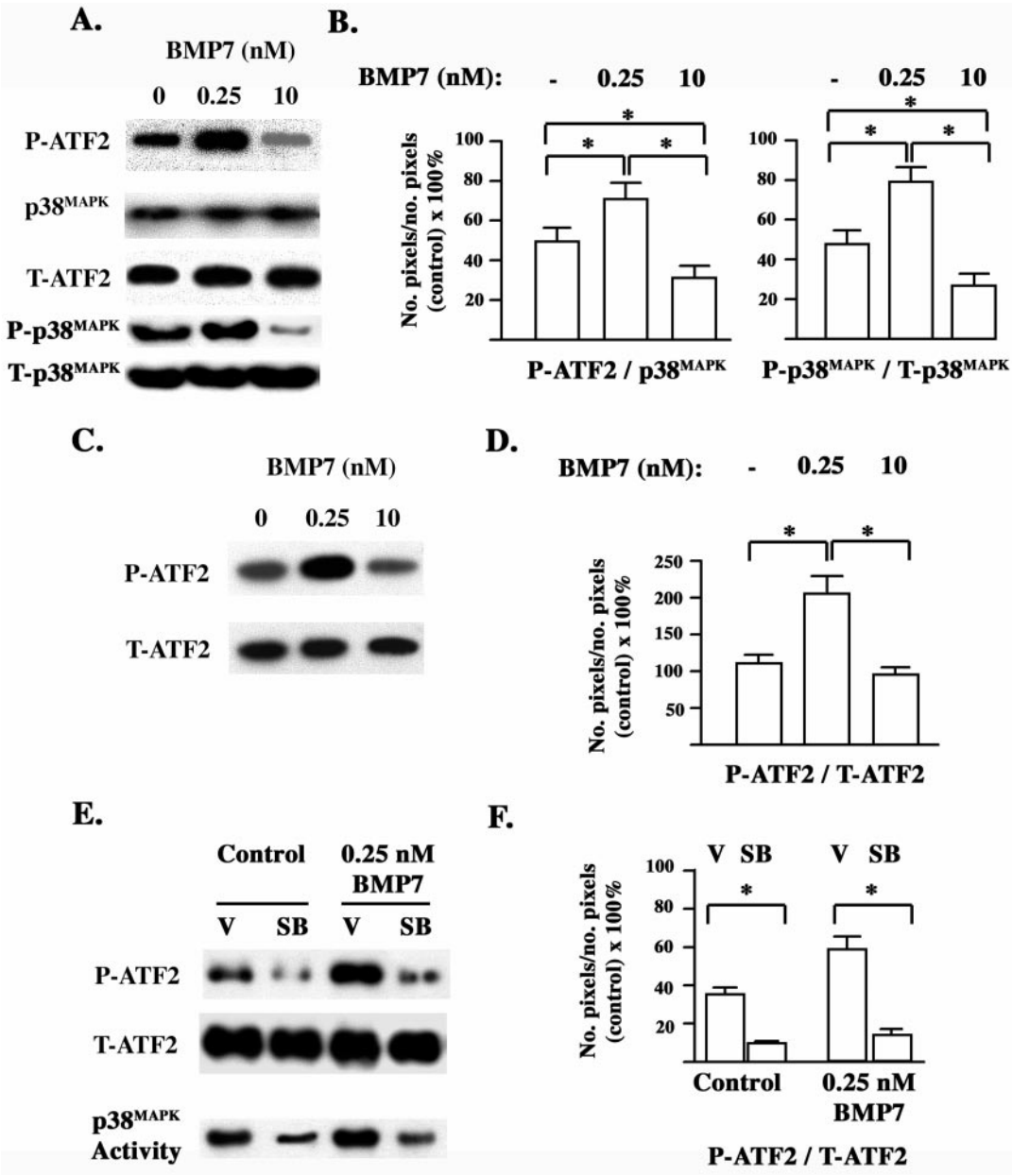

FIG. 1. **BMP7 increases phosphorylation of ATF2 in a p38^{MAPK}-dependent manner.** *A*, p38^{MAPK}-dependent phosphorylation of ATF2 and phosphorylation of p38^{MAPK} in BMP7-treated mIMCD-3 cells. p38^{MAPK} was isolated from cell lysates by immunoprecipitation and added to a kinase assay utilizing ATF2 as a substrate. P-ATF2, T-ATF2, and p38^{MAPK} were identified in immunoblots using specific antibodies. Phosphorylated (*P-p38^{MAPK}*) and total (*T-p38^{MAPK}*) forms of p38^{MAPK} were identified in cell lysates using specific antibodies. *B*, *left panel*, quantitation of P-ATF2 identified in *A*. The amount of P-ATF2 was controlled for the quantity of p38^{MAPK} in each sample. Low dose BMP7 stimulated p38^{MAPK}-dependent phosphorylation of ATF2. In contrast, high dose BMP7 was inhibitory. *, $p < 0.05$. $n = 6$ independent experiments. *Right panel*, quantitation of endogenous P-p38^{MAPK} identified in *A*. The amount of P-p38^{MAPK} was controlled for the quantity of T-p38^{MAPK} in each sample. Low dose BMP7 stimulated phosphorylation of p38^{MAPK}. In contrast, high dose BMP7 inhibited phosphorylation of p38^{MAPK}. *, $p < 0.05$. $n = 3$ independent experiments. *C*, levels of endogenous phosphorylated ATF2 (*P-ATF2*) in BMP7-treated mIMCD-3 cells. Proteins isolated from the cell lysates were analyzed with antibodies specific for phosphorylated ATF2 (*P-ATF2*), and total ATF2 (*T-ATF2*), consisting of both unphosphorylated and phosphorylated forms, by immunoblotting. *D*, quantitation of endogenous P-ATF2 detected in *C*. The amount of P-ATF2 was controlled for the quantity of T-ATF2 in each sample. Low dose BMP7 increased endogenous P-ATF2. *, $p < 0.0001$. $n = 4$ independent experiments. *E*, effect of SB203580 (*SB*) on BMP7-dependent phosphorylation of ATF2. mIMCD-3 cells were treated with or without BMP7 in the absence (vehicle (*V*) only) or presence of 1 μM SB203580. Endogenous P-ATF2 and T-ATF2 were detected in immunoblots using specific antisera. p38^{MAPK} activity was measured using a kinase assay as in *A*. *F*, quantitation of endogenous P-ATF2 detected in *E*. The amount of P-ATF2 was controlled for the quantity of T-ATF2 in each sample. Treatment with SB203580 decreased the basal levels of endogenous P-ATF2 and blocked the increase in P-ATF2 observed after treatment with 0.25 nM BMP7. *, $p < 0.05$. $n = 4$ independent experiments.

an inhibitory dose (10 nM) of BMP7 inhibited phosphorylation of p38^{MAPK} 1.7-fold compared with control and 2.9-fold compared with 0.25 nM BMP7 (P-p38^{MAPK} (densitometric units), control *versus* 0.25 nM BMP7, 48 ± 7 *versus* 78 ± 7, $p < 0.0001$; control *versus* 10 nM BMP7, 48 ± 7 *versus* 27 ± 5, $p < 0.0001$). Taken together, these results indicate that BMP7 modulates p38^{MAPK} activity in a biphasic dose-dependent manner.

Next, we determined whether BMP7 modulates the activity of endogenous ATF2. By using antibodies specific for the phosphorylated (activated) form of ATF2 and both phosphorylated and unphosphorylated (total) forms of ATF2, we detected endogenous phosphorylated and total ATF2 in immunoblots of cellular proteins isolated after treatment with recombinant BMP7. A stimulatory dose (0.25 nM) of BMP7 increased the

quantity of phospho-ATF2 2-fold (Fig. 1, *C* and *D*) (endogenous P-ATF2 (densitometric units), untreated *versus* 0.25 nM BMP7, 109 ± 17 *versus* 213 ± 23, $p < 0.0001$). In contrast, an inhibitory dose (10 nM) of BMP7 had no significant effect on phospho-ATF2 levels (Fig. 1, *C* and *D*) (endogenous P-ATF2 (densitometric units), untreated *versus* 10 nM BMP7, 109 ± 17 *versus* 83 ± 18, $p = 0.09$). Analysis of total ATF2 in each treatment group demonstrated that these results were not due to an effect of BMP7 on the total amount of ATF2 expressed in mIMCD-3 cells.

To determine whether BMP7 activates ATF2 via p38^{MAPK}, we measured the cellular levels of phospho-ATF2 in the presence or absence of SB203580, a pharmacologic p38^{MAPK} inhibitor (18). Treatment with SB303580 decreased the basal levels of endogenous P-ATF2 2.3-fold and abrogated the increase in P-ATF2 observed after treatment with low dose (0.25 nM) BMP7 (Fig. 1, *E* and *F*, P-ATF2/T-ATF2 (densitometric units), vehicle *versus* SB203580, 37 ± 12 *versus* 16 ± 8, $p = 0.01$; 0.25 nM BMP7 *versus* 0.25 nM BMP7 and SB203580, 60 ± 10 *versus* 18 ± 3, $p < 0.01$). Taken together, these results demonstrate that low doses of BMP7 stimulate phosphorylation of ATF2 in a p38^{MAPK}-dependent manner.

BMP7 Does Not Control SAPK/JNK and ERK Activity in Collecting Duct Cells—To determine whether the effects of BMP7 are specific to the p38 branch of the MAPK family, we measured SAPK/JNK and ERK1/2 activation in the presence of low and high doses of BMP7. A possible role for these kinases in BMP7 signaling is suggested by the previous findings that JNK and ERK are activated by BMPs in nonrenal cells (19) and that ERK acts downstream of non-BMP growth factors including hepatocyte growth factor and EGF to control epithelial morphogenesis (20). By using antibodies specific for the phosphorylated (active) forms of SAPK/JNK, phospho-p54 and phospho-p46, and ERK, phospho-p44 and phospho-p42, and both phosphorylated and unphosphorylated forms (total) of these proteins, we detected endogenous proteins in immunoblots of cellular proteins after treatment with low or high doses of BMP7 (Fig. 2, *A* and *B*). Our results indicate no significant effect of BMP7 on SAPK/JNK or ERK activation, thus demonstrating a specific effect of BMP7 on p38^{MAPK}.

Inhibition of p38^{MAPK} Blocks BMP7-mediated Stimulation of Collecting Duct Cell Morphogenesis—By having determined that BMP7 stimulates and inhibits p38^{MAPK} in a dose-dependent manner reminiscent of its actions during epithelial morphogenesis, we analyzed p38^{MAPK} function by inhibiting p38 pharmacologically in the mIMCD-3 culture model of collecting duct cell morphogenesis. We have used mIMCD-3 cells, which are derived from the terminal inner medullary collecting duct of the SV40 transgenic mouse, to determine the effects of BMP7 on cellular morphogenesis and proliferation (4, 5, 7). mIMCD-3 cells were seeded in type I collagen, cultured for 48 h in the presence of a wide range of BMP7 doses with or without SB203580, and then imaged by DIC microscopy (Fig. 3*A*). Because we observed an effect on the number of tubular progenitors, observed in this assay as linear structures, we quantitated the number of these structures in different treatment groups (Fig. 3, *B* and *C*). Consistent with our previously published results, BMP7 increased the number of linear structures in a dose-dependent manner demonstrating maximal stimulation of 1.6-fold at a dose of 0.25 nM. This BMP7-dependent stimulatory effect was ~3-fold less potent that that observed after treatment with EGF. The greater potency of EGF may due to its property of stimulating both ERK and p38^{MAPK} (21, 22). In contrast, BMP7, at doses greater than 1 nM, inhibited with a maximal inhibitory effect of 1.5-fold at a dose of 20 nM (Fig. 3, *A* and *B*). Remarkably, SB203580 totally abrogated the

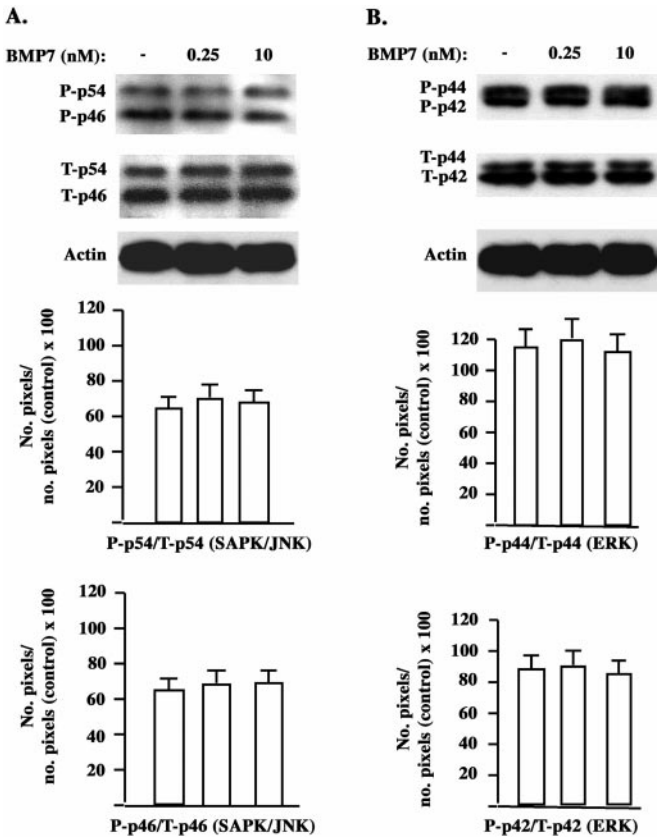

FIG. 2. **Effect of BMP7 on SAPK/JNK and ERK activation.** *A*, phosphorylation of p54 and p46 SAPK/JNK in BMP7-treated mIMCD-3 cells. *Upper panel*, proteins isolated from cell lysates were analyzed with antibodies specific for phosphorylated (*P-p54* and *P-p46*) and total p54 and p46 by immunoblotting. *Lower panels,* quantitation of endogenous P-p54 and P-p46, identified in *A.* The amount of P-p54 and P-p46 was controlled for the quantity of total p54 and total p46, respectively, in each sample. Low and high doses of BMP7 exerted no significant effect on the levels of endogenous P-p54 and P-p46. *B*, phosphorylation of p44 and p42 ERK in BMP7-treated mIMCD-3 cells. *Upper panel*, proteins isolated from cell lysates were analyzed with antibodies specific for phosphorylated (*P-p44* and *P-p42*) and total p44 and p42 by immunoblotting. *Lower panels*, quantitation of endogenous P-p44 and P-p42, identified in *A.* The amount of P-p44 and P-p42 was controlled for the quantity of total p44 and total p42, respectively, in each sample. Low and high doses of BMP7 exerted no significant effect on the levels of endogenous P-p44 and P-p42 ERK. $n = 4$ independent experiments.

stimulatory effects of BMP7 on mIMCD-3 cell morphogenesis but did not interfere with the inhibitory effects of BMP7 (Fig. 3*C*). The lack of any BMP7-dependent stimulatory response in the presence of SB203580 demonstrates that p38^{MAPK} is required for the stimulatory effects of BMP7.

In addition to the inhibitory effect of SB203580 on BMP7-dependent stimulation of mIMCD-3 cell morphogenesis, we observed a 25% decrease in the number of linear structures formed in the presence of SB203580 alone (Fig. 3, *B versus C*, 100 *versus* 78 tubule progenitors) and a diminished morphogenetic response to EGF in the presence of SB203580 (Fig. 3, *B versus C*, 480 *versus* 340 tubule progenitors). Although the observation that p38^{MAPK} is activated by EGF in nonrenal cells (22) may explain the decreased morphogenetic activity of mIMCD-3 cells cultured in the presence of SB203580, our data do not eliminate the possibility that SB203580 exerts a more general toxic effect on cellular function impacting negatively on mIMCD-3 cell morphogenesis.

ALK2 Inhibits Collecting Duct Cell Morphogenesis in a Ligand-independent Manner—Doses of BMP7 >1 nM exert a dominant inhibitory effect on p38^{MAPK} activation and collect-

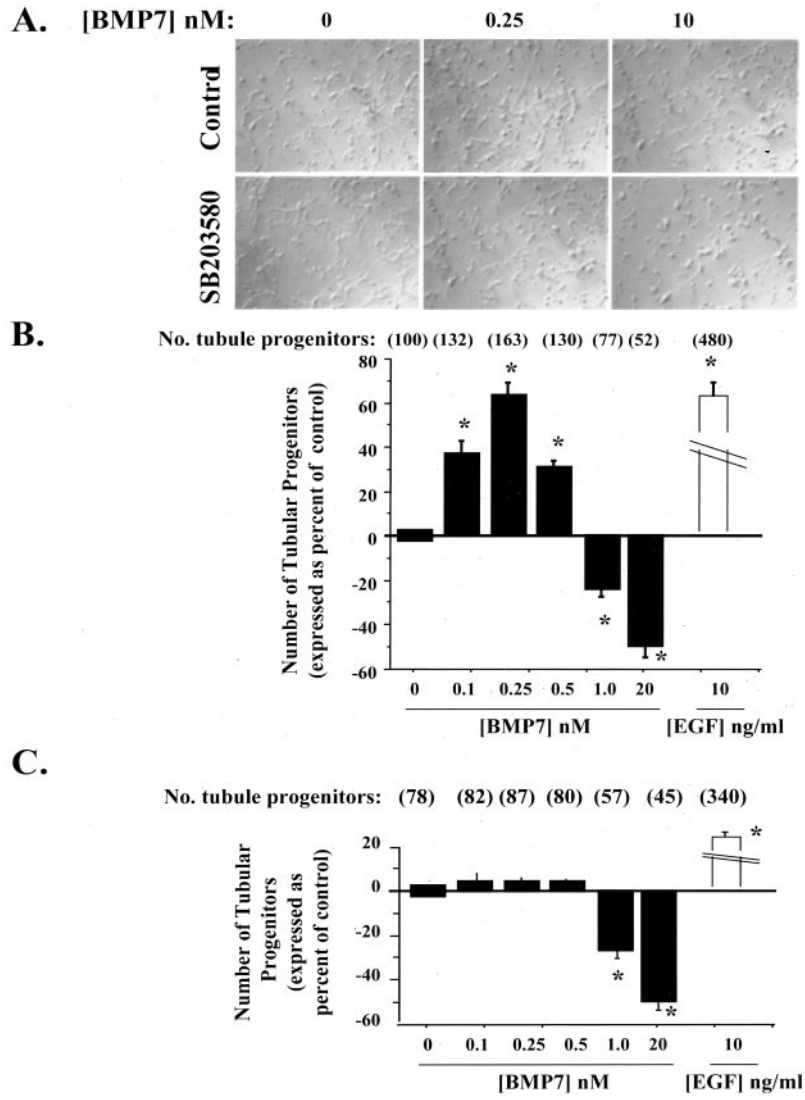

FIG. 3. **The p38^{MAPK} inhibitor, SB203580, blocks BMP7-dependent stimulation of collecting duct cell morphogenesis.** *A*, differential interference contrast images of mIMCD-3 cell structures formed 48 h after cultures were established (magnification = ×100). *B* and *C*, quantitation of the number of tubule progenitors (linear structures) formed by mIMCD-3 cells. The number of linear structures present in four randomly selected microscopic fields is shown in *parentheses above each bar*. The *bar graph* shows the number of structures formed in each treatment group as a % of control (no BMP7). *B*, mIMCD-3 cells were treated with increasing doses of BMP7 or EGF. BMP7 stimulated formation of linear structures maximally at a dose of 0.25 nM and inhibited at doses of 10 and 20 nM. *C*, mIMCD-3 cells were treated with increasing doses of BMP7 in the presence of 1 μM SB203580. The stimulatory response to BMP7 was blocked. In contrast, the inhibitory response to BMP7 was unaffected. *, $p < 0.01$. $n = 3$ independent experiments.

ing duct cell morphogenesis (see above and Ref. 5). We hypothesized that this dominance may be explained by negative regulation of p38^{MAPK} activity by Smad1 because high doses, but not low doses of BMP7, act via Smad1 (5). To study interactions between Smad and p38^{MAPK} signaling, we generated a ligand-independent model of ALK signaling designed to avoid potentially confounding effects of BMP7 signaling via both pathways. The ALK receptor, ALK2, binds BMP7 and activates Smad1 signaling (23). A mutant ALK2 allele, *Alk2^{Q207D}*, is characterized by a point mutation in its cytoplasmic GS domain and constitutively activates Smad1 in a ligand-independent manner (24). We generated stably transfected mIMCD-3 cell lines expressing tagged versions of wild-type ALK2 and ALK2^{Q207D}, both of which were detected as a 68-kDa band by Western analysis using anti-FLAG monoclonal antibody (Fig. 4*A*). Several different clones were isolated. Clones expressing high levels of ALK2^{WT} (clone 42) or ALK2^{Q207D} (clone 26) were analyzed further first by examining the subcellular distribution of ALK3-HA-FLAG using immunofluorescence and confocal microscopy (Fig. 4*B*). In contrast to untransfected mIMCD-3 cells, we observed a punctate pattern of expression along the border of 81% of cells stably expressing ALK2^{WT} and 86% of cells stably expressing ALK2^{Q207D}. This pattern was consistent with localization of the transfected ALK2 to the peripheral cell membranes.

Next, we determined the functional effects of ALK2^{Q207D} expression on Smad signaling by using an assay of Smad1-Smad4 molecular complex formation (Fig. 4*C*). Smad1-Smad4 molecular complexes were detected at very low levels under basal conditions in ALK2^{WT}-expressing cells. In contrast, these complexes were undetectable in unstimulated mIMCD-3 cells. This difference is consistent with the prior observation that overexpression of wild-type type I BMP receptors can lead to autoactivation of receptors on the cell surface (14). Treatment of ALK2^{WT}-expressing cells with 20 nM BMP7 resulted in the formation of Smad1-Smad4 molecular complexes as observed in mIMCD-3 cells. In ALK2^{Q207D}-expressing cells, we detected high levels of Smad1-Smad4 molecular complexes under basal conditions (no ligand). This result was consistent with constitutive signaling by the mutant ALK2 receptor. The amount of Smad4 detected in association with Smad1 was increased after treatment with high dose BMP7 suggesting enhanced signaling via endogenous wild-type ALK2 or another ALK receptor. Our demonstration that equivalent amounts of Smad4 and Smad1 were expressed in ALK2^{WT}- and ALK2^{Q207D}-expressing cells indicates that these differences in Smad4 associated with Smad1 are not due to differences in the absolute amounts of Smad1 and Smad4 expressed in these cells.

We further investigated ALK2^{Q207D} function by investigating its effects on BMP7-dependent collecting cell morphogenesis in the mIMCD-3 cell culture model (Fig. 5). First, we ana-

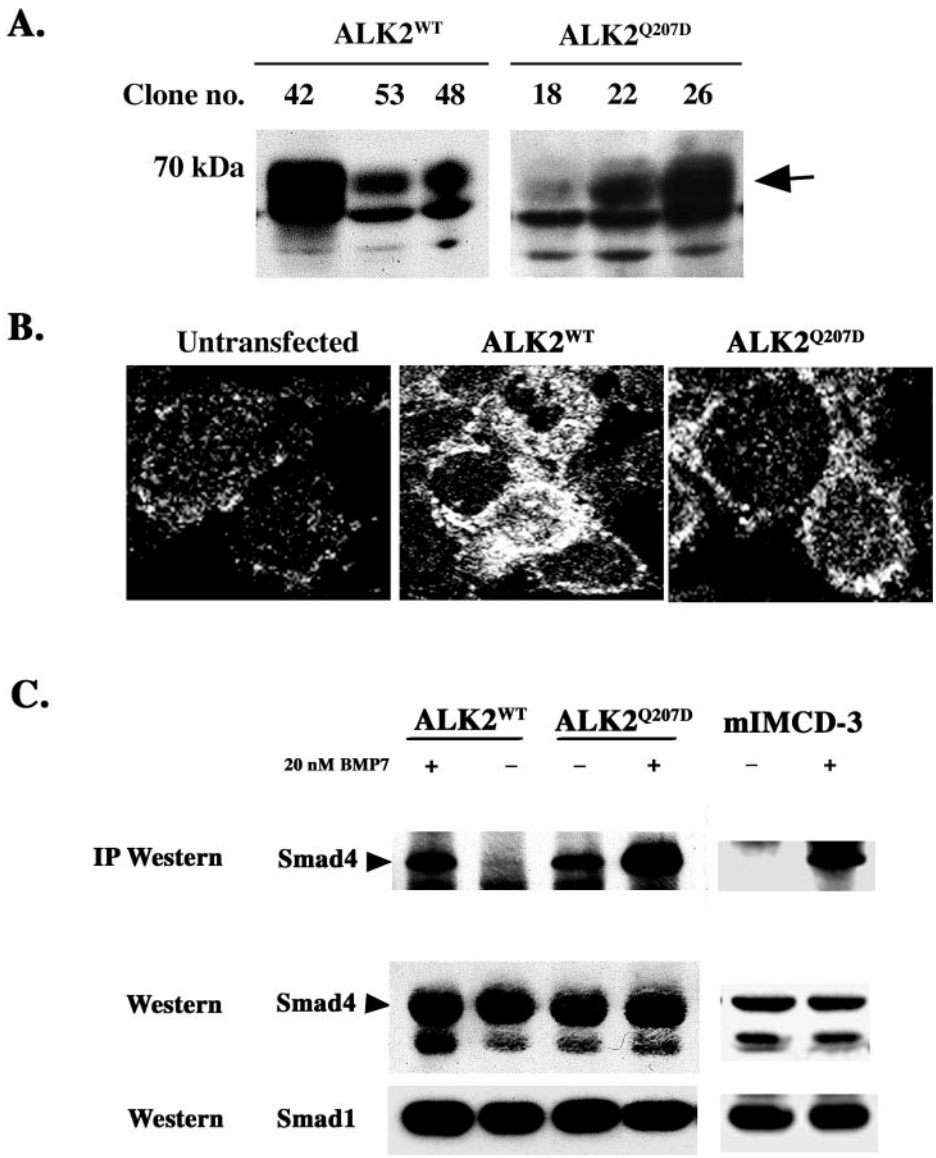

FIG. 4. **Expression of a constitutive active *Alk2* allele induces formation of Smad1-Smad4 molecular complexes in mIMCD-3 cells.** *A*, mIMCD-3 cells were stably transfected with plasmids encoding FLAG-HA-tagged WT or Q207D forms of *Alk2*. Proteins from cell lysates were analyzed by immunoblotting using an anti-FLAG antibody. Several clones differing in the quantity of tagged-ALK2 expressed were isolated. *B*, FLAG-HA-tagged ALK2^{WT} clone 42 and ALK2^{Q207D} clone 26 were grown in monolayer. HA was detected by confocal laser microscopy using a mouse monoclonal anti-HA antibody and a fluorescein-conjugated secondary antibody (×480 magnification). *C*, ALK2^{WT} and ALK2^{Q207D} clones and untransfected mIMCD-3 cells were treated for 1 h with either no ligand or 20 nM BMP7. Proteins in cell lysates were immunoprecipitated (*IP*) with an antibody to Smad1, separated by SDS-PAGE, and then analyzed by Western blotting using an antibody to Smad4. The quantity of Smad1 and Smad4 in each assay was analyzed by immunoblotting. Smad1-Smad4 molecular complexes were detected at very low levels in ALK2^{WT} cells under basal conditions and in untransfected mIMCD-3 cells only after treatment with 20 nM BMP7. In contrast, these complexes were detected in ALK2^{Q207D} cells in the absence of ligand. $n = 3$ independent experiments.

lyzed whether overexpression of ALK2 disrupted the dose-response to BMP7 by treating ALK2^{WT}-expressing cells with increasing doses of BMP7 and counting the number of linear structures formed (Fig 5, *A* and *B*). Although we observed a decrease in the absolute number of tubule progenitors consistent with our previous results in mIMCD-3 cells transfected with wild-type ALK3 (8) and wild-type Smad1 (5), the dose-dependent stimulatory and inhibitory responses to BMP7 were intact. In contrast, ALK2^{Q207D}-expressing cells demonstrated a persistent "inhibitory" tubulogenic profile compared with ALK2^{WT}-expressing cells (Fig. 5, *A* and *C*). The number of tubule progenitors formed by ALK2^{Q207D}-expressing cells under basal conditions was less than one-half that observed in cultures of ALK2^{WT}-expressing cells (Fig. 5, *C versus B*). In addition, ALK2^{Q207D}-expressing cells were unresponsive to stimulatory doses of BMP7 (Fig. 5, *A* and *C*). Yet formation of tubule progenitors could be stimulated with EGF, demonstrating the viability of these cells. However, the decreased number of tubule progenitors formed by ALK2^{Q207D} cells as compared with ALK2^{WT} cells in response to EGF indicated a dominant effect of Smad signaling over EGF signaling in a manner similar to the dominant effect of Smad signaling over hepatocyte growth factor signaling observed by us previously (8). Taken together, these results demonstrate that ALK2^{Q207D} signals via Smad1 and inhibits collecting duct cell morphogenesis in a ligand-independent manner.

Activation of Receptor-activated Smads Negatively Regulates p38^{MAPK}—We investigated interactions between the Smad signaling pathway and p38^{MAPK} in mIMCD-3 cells in which Smad signaling is enhanced or suppressed. In ALK2^{Q207D}-expressing cells, Smad1 signaling is up-regulated in a ligand-independent manner (see above and Fig. 4*C*). We measured p38^{MAPK}-dependent phosphorylation of ATF2 in mIMCD-3^{ALK2Q207D} cells in the absence of exogenous BMP7 (Fig. 6, *A* and *B*). p38^{MAPK}-dependent phosphorylation of ATF2 was decreased 1.8-fold, suggestive of a negative regulatory effect of Smad1 on p38^{MAPK} activity (p38^{MAPK} activity, control cells *versus* ALK2^{Q207D} cells, 118 ± 20 *versus* 68 ± 17, $p = 0.003$). Negative regulation of p38^{MAPK} by Smad1 predicted that p38^{MAPK} activity would be increased in cells with decreased Smad signaling. Previously, we demonstrated that stable expression of a dominant negative Smad1 allele, Smad1$^{\Delta 458}$, in mIMCD-3 cells decreased ligand-dependent activation of Smad1 (5). We measured p38^{MAPK} activity in mIMCD-3$^{Smad1\Delta 458}$ cells and demonstrated a 1.8-fold increase in p38^{MAPK}-dependent ATF2 phosphorylation (p38^{MAPK} activity, control cells *versus* Smad1$^{\Delta 458}$ cells, 118 ± 20 *versus* 210 ± 17, $p < 0.0001$). Taken together, these results

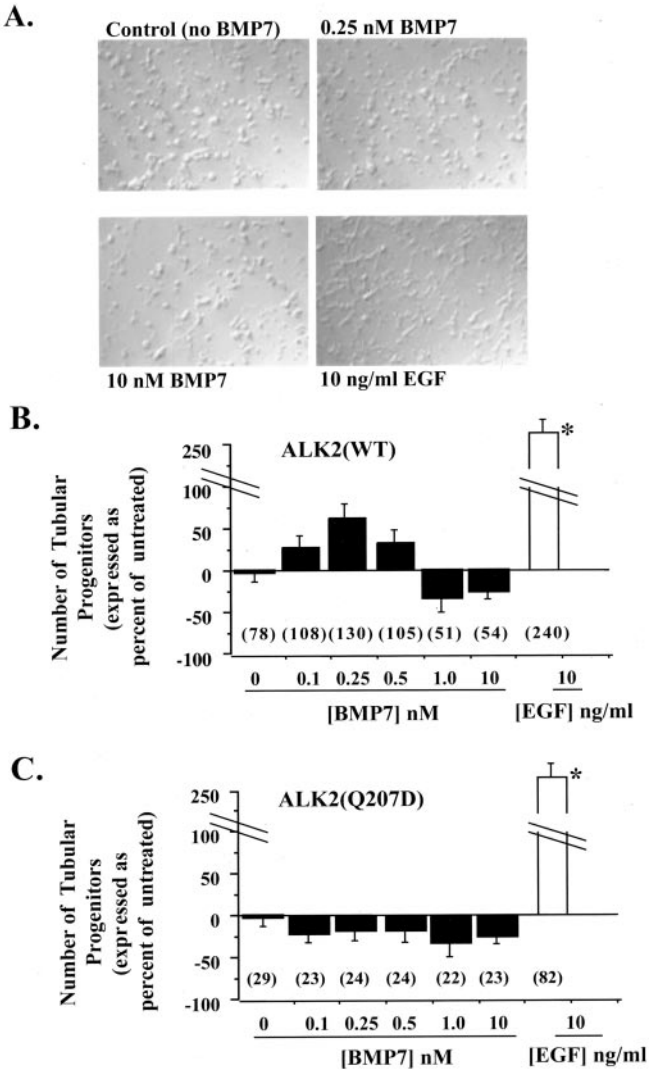

FIG. 5. **mIMCD-3 cells stably expressing ALK2^{Q207D} exhibit an inhibitory phenotype when induced to form tubule progenitors.** mIMCD-3 cells expressing ALK2^{Q207D} were cultured for 48 h in type I collagen with culture medium supplemented with either no ligand, BMP7, or EGF. *A*, structures formed were imaged by DIC microscopy (×100 magnification). *B* and *C*, quantitation of effects of BMP7 on formation of tubule progenitors by mIMCD-3 cells expressing ALK2^{WT} or ALK2^{Q207D}. The number of linear structures present in four randomly selected microscopic fields is shown in *parentheses below each bar*. The *bar graph* shows the number of structures formed in each treatment group as a % of control (no BMP7). *B*, stable expression of ALK2^{WT} decreased the absolute number of tubule progenitors but did not interfere with the dose-dependent stimulatory and inhibitory effects of BMP7. *C*, stable expression of ALK2^{Q207D} inhibited in a manner identical to treatment with high doses of BMP7. *, $p < 0.05$. $n = 3$ independent experiments.

indicate that Smad1 activity is inversely related to p38^{MAPK} activity in mIMCD-3 cells.

Phosphorylation of ATF2 Is Decreased in Embryonic Kidney Tissue Expressing a Constitutive Active ALK3 Receptor—Our results indicating interactions between Smad1 and p38^{MAPK} signaling in collecting duct cells suggested that Smad1 may regulate p38^{MAPK} activity in renal cells *in vivo*. Because both Smad1 and p38^{MAPK} are highly expressed at the time during which BMP7 is expressed in the embryonic kidney, Smad1-p38^{MAPK} interactions could serve as a mechanism to modulate the dose-dependent effects of BMP7 on tubular epithelial cells. We have reported the functions of ALK3, a receptor that signals via Smad1 (8), during kidney development in transgenic mice expressing the constitutive active receptor, ALK3^{Q233D} (25). Consistent with the effects of ALK2 in mIMCD-3 cell cultures, a decreased number of ureteric bud branches, identified by *D. biflorus* agglutinin, were formed in the kidneys of ALK3 transgenic mice compared with those of control mice (number branch points, *Alk3^{Q233D} versus* control, 33 ± 4 *versus* 42 ± 5, $p < 0.05$) (Fig. 6*C*) (25). We analyzed ATF2 activity by measuring the levels of endogenous phosphorylated ATF2 in protein lysates generated from the kidneys isolated from E13.5 ALK3 transgenic and control mice. Our results demonstrate a 1.4-fold decrease in phosphorylated ATF2 in kidneys from ALK3 transgenic mice (Fig 6, *C* and *D*) (endogenous ATF2 (densitometric units), control *versus Alk3* transgenic mice, 64 ± 3 *versus* 46 ± 8, $p = 0.007$). These findings suggest that signaling via ALK receptors negatively regulates ATF2 activity. These results, together with those in mIMCD-3 cells, suggest a model of Smad1-p38^{MAPK} interactions in which ALK-dependent activation of Smad1 negatively regulates p38^{MAPK} resulting, in turn, in decreased ATF2 activity.

DISCUSSION

The arrest of branching morphogenesis observed in the dysplastic kidneys of *Bmp7* null mice provides compelling evidence that BMP7 is required for normal renal development (2, 3). Our previous demonstration that recombinant BMP7 exerts dose-dependent stimulatory and inhibitory effects on renal branching morphogenesis suggested the existence of distinct signaling pathways that transduce these effects (4). This dual signaling model was strengthened by our results indicating differential signaling by high and low doses of BMP7 via Smad1. High doses (≥0.5 nM) of BMP7 require Smad1 to inhibit tubule growth and branching. In contrast, low doses (<0.5 nM) of BMP7 stimulate these processes in a Smad1-independent manner (5). In this work, we further elucidate the mechanisms controlling dose-dependent signaling BMP7. We demonstrate a distinct and novel role for p38^{MAPK} in BMP7-dependent stimulation. Doses of BMP7 that stimulate collecting duct cell morphogenesis stimulated p38^{MAPK} activity. In contrast, doses of BMP7 that inhibit epithelial cell morphogenesis inhibit inhibited p38^{MAPK}. Furthermore, we show that BMP7 regulates the phosphorylation of endogenous ATF2 in a p38^{MAPK}-dependent manner. The functional significance of these results was investigated in the mIMCD-3 culture model in which we demonstrated that pharmacologic inhibition of p38^{MAPK} activity blocks BMP7-dependent stimulation of mIMCD-3 cell morphogenesis but does not affect BMP7-dependent inhibition.

Our results demonstrate opposing functions for p38^{MAPK} and BMP-activated Smads in collecting duct cells. p38^{MAPK}-Smad interactions have been investigated previously in non-renal cells. The majority of studies have focused on the effects of TGF-β. Evidence supporting cooperative interactions includes the finding that TGF-β induces phosphorylation of ATF2 in a p38^{MAPK}-dependent manner and formation of ATF2-Smad4 molecular complexes (17). In prostatic epithelial cells, p38^{MAPK} is required for TGF-β- and Smad3-dependent cell adhesion and nuclear translocation of Smad3 (26). In human epithelial cells, ATF3 and Smad3 act cooperatively to control Id1 promoter activity (27). In gingival fibroblasts, p38^{MAPK} and Smad3 act cooperatively to control collagenase-3 gene expression, and nuclear translocation of Smad3 is dependent on p38^{MAPK} activity (28). In cultured pancreatic cells, TGF-β or an activated TGF-β-responsive ALK receptor can activate p38^{MAPK} and Smad3 is required for p38^{MAPK} activation (29).

A limited number of studies have investigated interactions between BMP-dependent Smad signaling and p38^{MAPK}. BMP-activated Smads and ATF2 act cooperatively to control β-myosin heavy chain gene expression and cardiomyocyte differenti-

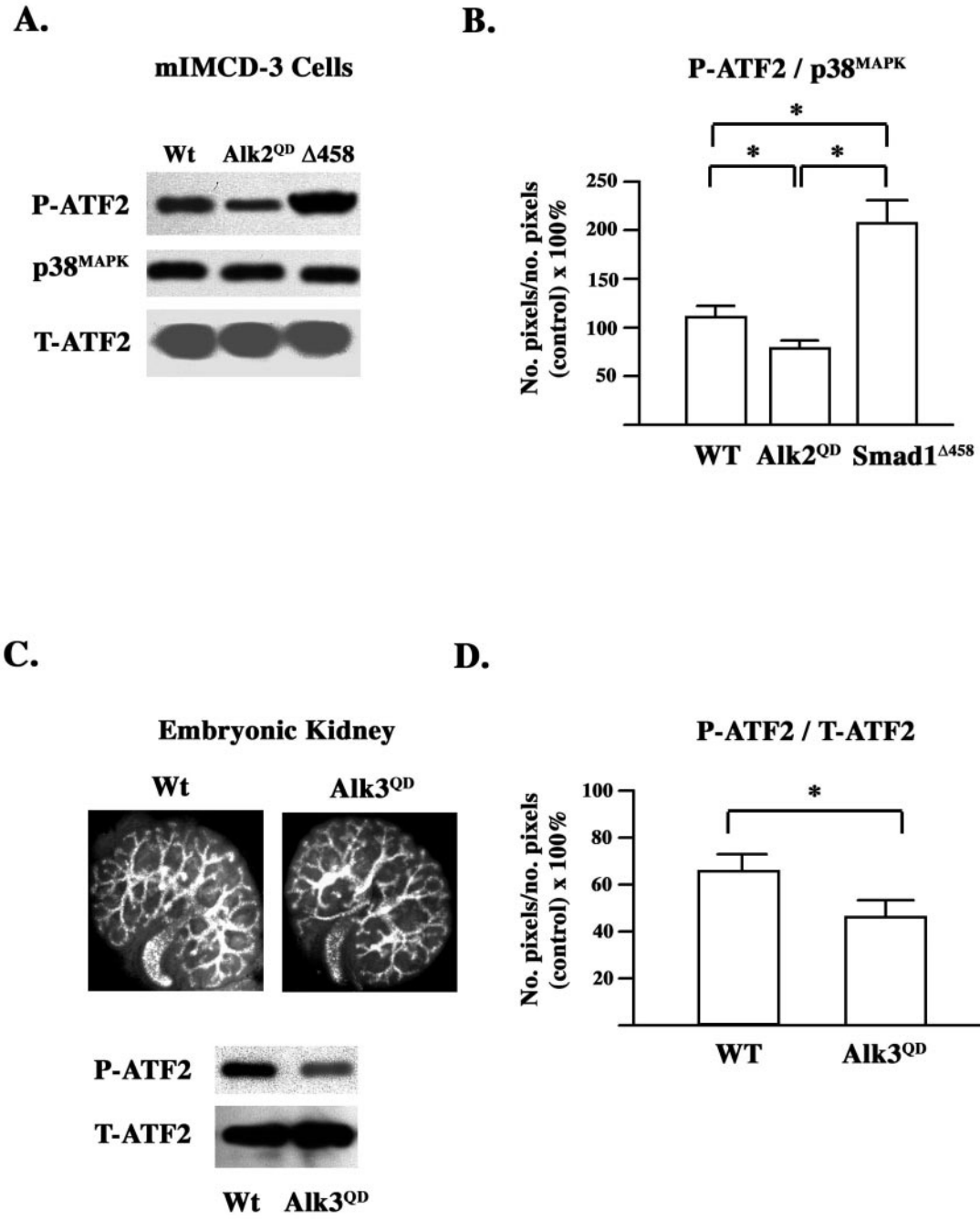

FIG. 6. **The activity of p38^{MAPK} and ATF2 is regulated by ALK/Smad signaling.** *A*, p38^{MAPK}-dependent phosphorylation of ATF2 was measured in wild-type mIMCD-3 cells and in mIMCD-3 cells stably expressing ALK2^{Q207D} or a dominant negative acting Smad1 allele (Smad1$^{\Delta 458}$). P-ATF2, T-ATF2, and p38^{MAPK} were detected in protein lysates using specific antibodies. *B*, quantitation of P-ATF2 detected in *A.* The amount of P-ATF2 was controlled for the quantity of immunoprecipitated p38^{MAPK} in each sample. p38^{MAPK}-dependent phosphorylation of ATF2 was suppressed by stable expression of ALK2^{Q207D} and was enhanced by expression of Smad1$^{\Delta 458}$. *, $p < 0.005$. $n = 4$ independent experiments. *C*, *top*, immunofluorescence images of whole mount preparations of embryonic kidneys isolated from control and *Alk3* transgenic mice at E13.5. Ureteric bud branches are stained with *D. biflorus* agglutinin. *Bottom*, immunoblots of tissue protein lysates generated from kidneys of E13.5 mice. *D*, quantitation of P-ATF2 detected in *C.* The amount of P-ATF2 was controlled for the quantity of T-ATF2 in each sample. The level of endogenous P-ATF2 was suppressed in the embryonic kidneys of *Alk3* transgenic mice, isolated at the stage of branching morphogenesis. *, $p < 0.01$. $n = 4$ independent experiments.

ation (30). A study of peroxisome proliferator-activated receptor-γ regulation during adipogenesis shows that both BMP2 and p38^{MAPK} act cooperatively during the differentiation of undifferentiated mesenchymal cells into adipocytes. However, the role of Smad1 in BMP2-dependent p38^{MAPK} activation was not addressed directly (31).

In contrast to these studies, others that show TGF-β-dependent induction of Smad and p38^{MAPK} signaling do not demonstrate a dependence of p38^{MAPK} effects on Smads and vice versa. Expression of a dominant negative form of Smad3 or the ALK inhibitor, Smad7, did not interrupt TGF-β-dependent p38^{MAPK} activation in NMuMG mammary epithelial cells (32). Similarly, in the MDA-231 cell model of breast cancer, both TGF-β and p38^{MAPK} control expression of parathyroid hormone-related protein, but p38^{MAPK} activation is not Smad-dependent (33). Taken together, these studies consistently demonstrate that TGF-β and BMP2 activate both Smad- and p38^{MAPK}-dependent signaling pathways. However, the interdependency

of these pathways appears to be due, in part, to the cellular context in which signaling is initiated.

Although our study provides additional insight into the interplay between p38^{MAPK} and Smad signaling, it does not address the molecular mechanism that transduces BMP7-dependent activation of p38^{MAPK} distinct from Smad activation. It is possible that the dose-dependent effects of BMP7 might be explained by binding to distinct ALK receptors in a manner dependent on the dose of BMP7. Such a model would further suggest that distinct ALK receptors have differential activity in activating Smads and p38^{MAPK}. Previous work (34) has shown that BMP7 binds to ALK2, ALK3, and ALK6 with different affinities. Each of these ALK receptors has been demonstrated to signal via the Smad pathway. Furthermore, a study of TGF-β-dependent activation of p38^{MAPK} in which a mutant TGF-β-binding ALK receptor that cannot bind Smads but retains kinase activity demonstrated that ligand-dependent activation of p38^{MAPK} was not interrupted (32). Thus, it is possible that ALK receptors transduce signals to both p38^{MAPK} and Smads but that the kinetics of p38^{MAPK} and Smad activation are dependent on the dose of ligand presented to the receptor. Recent studies have suggested a possible mechanism by which BMP7 could trigger p38^{MAPK} at doses lower than those required for Smad activation. In C2C12 and MC3T3 cells, BMP heteromeric complexes exist on the cell surface in the absence of ligand (35). Ligand binding to these preformed complexes triggers Smad activation. In contrast, receptor complexes that form only upon interaction with ligand trigger p38^{MAPK}-dependent signaling (36). These observations raise the possibility that different doses of BMP7 differentially engage preformed *versus* ligand-stimulated receptor complexes. Alternatively, activation of p38^{MAPK} by low doses of BMP7 may be independent of ALK receptor activation. Studies of BMP7 signaling in osteoblastic cells demonstrate that up-regulation of alkaline phosphatase, a p38^{MAPK} target, is blocked by antibodies directed against α_1 and α_2 integrins (37). These results suggest that BMP7 bound to integrins could trigger p38^{MAPK} activation. Further studies will be required to test elements of these signaling models.

We have proposed previously (5) that BMP7 acts in a dose-dependent activity gradient to control rates of cell proliferation, tubule growth, and branching during kidney development. This hypothesis is based on our findings that BMP7 controls ureteric bud and collecting duct branching and cell proliferation in a dose-dependent manner and that cell proliferation in these tubules is spatially regulated. The studies reported here suggest a model in which differential cellular responses within a BMP7 concentration gradient are controlled by distinct signaling pathways. The p38^{MAPK} pathway would control responses to low doses of BMP7 leading to increased cell proliferation and branching whereas the Smad pathway would control responses to high doses of BMP7 suppressing cell proliferation and branching. Suppression of p38^{MAPK} activity by high doses of BMP7 would serve to integrate the dose-dependent cellular response to BMP7.

Acknowledgments—We thank Yunkai Yu for expert technical assistance with these studies and Drs. Howard Lipshitz, Benjamin Alman, and C.-C. Hui for helpful discussions.

REFERENCES

1. Dudley, A. T., and Robertson, E. J. (1997) *Dev. Dyn.* **208,** 349–362
2. Dudley, A. T., Lyons, K. M., and Robertson, E. J. (1995) *Genes Dev.* **9,** 2795–2807
3. Luo, G., Hofmann, C., Bronckers, A. L. J. J., Sohocki, M., Bradley, A., and Karsenty, G. (1995) *Genes Dev.* **9,** 2808–2820
4. Piscione, T. D., Yager, T. D., Gupta, I. R., Grinfeld, B., Pei, Y., Attisano, L., Wrana, J. L., and Rosenblum, N. D. (1997) *Am. J. Physiol.* **273,** F961–F975
5. Piscione, T. D., Phan, T., and Rosenblum, N. D. (2001) *Am. J. Physiol.* **280,** F19–F33
6. Hoodless, P. A., Haerry, T., Abdollah, S., Stapleton, M., O'Connor, M. B., Attisano, L., and Wrana, J. L. (1996) *Cell* **85,** 489–500
7. Gupta, I. R., Piscione, T. D., Grisaru, S., Phan, T., Macias-Silva, M., Zhou, X., Whiteside, C., Wrana, J. L., and Rosenblum, N. D. (1999) *J. Biol. Chem.* **274,** 26305–26314
8. Gupta, I. R., Macias-Silva, M., Kim, S., Zhou, X., Piscione, T. D., Whiteside, C., Wrana, J. L., and Rosenblum, N. D. (2000) *J. Cell Sci.* **113,** 269–278
9. Lee, K. S., Hong, S. H., and Bae, S. C. (2002) *Oncogene* **21,** 7156–7163
10. Iwasaki, S., Iguchi, M., Watanabe, K., Hoshino, R., Tsujimoto, M., and Kohno, M. (1999) *J. Biol. Chem.* **274,** 26503–26510
11. Kimura, N., Matsuo, R., Shibuya, H., Nakashima, K., and Taga, T. (2000) *J. Biol. Chem.* **275,** 17647–17652
12. Omori, S., Hida, M., Ishikura, K., Kuramochi, S., and Awazu, M. (2000) *Kidney Int.* **58,** 27–37
13. Hida, M., Omori, S., and Awazu, M. (2002) *Kidney Int.* **61,** 1252–1262
14. Attisano, L., Carcamo, J., Ventura, F., Weis, F. M., Massague, J., and Wrana, J. (1993) *Cell* **75,** 671–680
15. Grisaru, S., Cano-Gauci, D., Tee, J., Filmus, J., and Rosenblum, N. D. (2001) *Dev. Biol.* **230,** 31–46
16. Curthoys, N. P., and Gstraunthaler, G. (2001) *Am. J. Physiol.* **281,** F381–F390
17. Sano, Y., Harada, J., Tashiro, S., Gotoh-Mandeville, R., Maekawa, T., and Ishii, S. (1999) *J. Biol. Chem.* **274,** 8949–8957
18. Young, P. R. (1997) *J. Biol. Chem.* **272,** 12116–12121
19. Lai, C. F., and Cheng, S. L. (2002) *J. Biol. Chem.* **277,** 15514–15522
20. Karihaloo, A., O'Rourke, D. A., Nickel, C., Spokes, K., and Cantley, L. G. (2001) *J. Biol. Chem.* **276,** 9166–9173
21. Yamanaka, Y., Hayashi, K., Komurasaki, T., Morimoto, S., Ogihara, T., and Sobue, K. (2001) *Biochem. Biophys. Res. Commun.* **281,** 373–377
22. Neve, R. M., Holbro, T., and Hynes, N. E. (2002) *Oncogene* **21,** 4567–4576
23. Macías-Silva, M., Hoodless, P. A., Tang, S. J., Buchwald, M., and Wrana, J. L. (1998) *J. Biol. Chem.* **273,** 25628–25636
24. Carcamo, J., Weis, F. M. B., Ventura, F., Wieser, R., Wrana, J. L., Attisano, L., and Massague, J. (1994) *Mol. Cell. Biol.* **14,** 3810–3821
25. Hu, M. C., Piscione, T. D., and Rosenblum, N. D. (2003) *Development* **130,** 2753–2766
26. Hayes, S. A., Huang, X., Kambhampati, S., Platanias, L. C., and Bergan, R. C. (2003) *Oncogene* **22,** 4841–4850
27. Kang, Y., Chen, C. R., and Massague, J. (2003) *Mol. Cell* **11,** 915–926
28. Leivonen, S. K., Chantry, A., Hakkinen, L., Han, J., and Kahari, V. M. (2002) *J. Biol. Chem.* **277,** 46338–46346
29. Takekawa, M., Tatebayashi, K., Itoh, F., Adachi, M., Imai, K., and Saito, H. (2002) *EMBO J.* **21,** 6473–6482
30. Monzen, K., Hiroi, Y., Kudoh, S., Akazawa, H., Oka, T., Takimoto, E., Hayashi, D., Hosoda, T., Kawabata, M., Miyazono, K., Ishii, S., Yazaki, Y., Nagai, R., and Komuro, I. (2001) *J. Cell Biol.* **153,** 687–698
31. Hata, K., Nishimura, R., Ikeda, F., Yamashita, K., Matsubara, T., Nokubi, T., and Yoneda, T. (2003) *Mol. Biol. Cell* **14,** 545–555
32. Yu, L., Hebert, M. C., and Zhang, Y. E. (2002) *EMBO J.* **21,** 3749–3759
33. Kakonen, S. M., Selander, K. S., Chirgwin, J. M., Yin, J. J., Burns, S., Rankin, W. A., Grubbs, B. G., Dallas, M., Cui, Y., and Guise, T. A. (2002) *J. Biol. Chem.* **277,** 24571–24578
34. ten Dijke, P., Ichijo, H., Franzen, P., Schulz, P., Saras, J., Toyoshima, H., Heldin, C.-H., and Miyazono, K. (1993) *Oncogene* **8,** 2879–2887
35. Gilboa, L., Nohe, A., Geissendorfer, T., Sebald, W., Henis, Y. I., and Knaus, P. (2000) *Mol. Biol. Cell* **11,** 1023–1035
36. Nohe, A., Hassel, S., Ehrlich, M., Neubauer, F., Sebald, W., Henis, Y. I., and Knaus, P. (2002) *J. Biol. Chem.* **277,** 5330–5338
37. Jikko, A., Harris, S. E., Chen, D., Mendrick, D. L., and Damsky, C. H. (1999) *J. Bone Miner. Res.* **14,** 1075–1083

$p38^{MAPK}$ Acts in the BMP7-dependent Stimulatory Pathway during Epithelial Cell Morphogenesis and Is Regulated by Smad1

Ming Chang Hu, David Wasserman, Sunny Hartwig and Norman D. Rosenblum

J. Biol. Chem. 2004, 279:12051-12059.
doi: 10.1074/jbc.M310526200 originally published online January 12, 2004
